academicJournals

Vol. 5(6), pp. 84-91, August 2014
DOI: 10.5897/JYFR2014.0137
Article Number: DD0FC4447270
ISSN 2141-2413

http://www.academicjournals.org/JYFR

Journal of Yeast and Fungal Research

Full Length Research Paper

Polycyclic aromatic hydrocarbons and small related molecules: Effects on *Schizosaccharomyces pombe* morphology measured by imaging flow cytometry

Trí Lê[1], Areeba Qureshi[1], Joel Heisler[1], Laura Bryant[1], Jehan Shah[1], Tom D. Wolkow[2] and Radha Pyati[1]*

[1]Department of Chemistry, University of North Florida, Jacksonville, FL 32224, U.S.A.
[2]Department of Biology, University of Colorado at Colorado Springs, Colorado Springs, Colorado, 80933, USA.

Received 30 May, 2014; Accepted 6 August, 2014

Effects of polycyclic aromatic hydrocarbons and small related molecules on the morphology of fission yeast (*Schizosaccharomyces pombe*) are described. Polycyclic aromatic hydrocarbons are important environmental pollutants that act as carcinogens via several mechanisms of action. Fission yeast is a useful model organism for revealing the mechanisms by which these molecules affect the cell. None of the molecules studied affected cell length of wildtype or a rad26Δ mutant yeast relative to control, indicating that none of these operate like known genotoxins that lengthen the cell. Five compounds are shown to decrease cell width in wildtype fission yeast, but not in the rad26Δ strain. These results indicate that machinery controlling the cell's width is affected by these molecules, and that this change is not detected when the rad26 protein is absent. These observations were made using imaging flow cytometry, which captures tens of thousands of two-dimensional cell images in a short time and provides statistically rigorous data on large cell populations.

Key words: Fission yeast, *Schizosaccharomyces pombe*, hydrocarbon, polycyclic aromatic hydrocarbon (PAH), morphology, imaging flow cytometry.

INTRODUCTION

Polycyclic aromatic hydrocarbons (PAHs) are an important group of persistent environmental pollutants generated by combustion and industrial processes and found in air, soil and water. Several PAHs have been identified as priority pollutants by the United States Environmental Protection Agency (USEPA, 2014). They have also been found in tobacco smoke and its extract (Talhout, 2011).

PAHs have been shown to act as carcinogens, and they operate by a variety of mechanisms. One of the importance of these is that they form DNA-adducts, in which the PAH covalently binds to DNA, affecting its replication (Beland, 1994). Another pathway is the activation of the aryl hydrocarbon signaling receptor.

*Corresponding author. E-mail: radha.pyati@unf.edu. Tel: +1-904-620-1918.

While this step is usually the initial activating factor that makes a PAH available to form a DNA adduct, this step also has been shown to have other effects on cellular growth and proliferation (Chramostova, 2004). A third pathway is the generation by PAHs of reactive oxygen species that cause oxidative stress (Munoz, 2011). Often these mechanisms work synergistically (Rubin, 2001) or against each other, and separating the threads of causality is an ongoing focus of research.

Examining PAH mechanisms of action has been done in several cell types and organisms, including *Saccharomyces cerevisiae* (Siebert, 1981; Deng, 2010; Alnafisi, 2007). As well, the effects of whole tobacco smoke extract, which contains several PAHs, on fission yeast (*Schizosaccharomyces pombe*) have been characterized in detail (Chaudhuri, 2005; Sundaram, 2008a, b). However, there is no systematic study of PAHs in fission yeast in the literature.

Fission yeast is a simple and useful model to study cellular processes. It possesses many genes similar to human genes, and processes affecting many types of human cells and instrumental in disease have been studied in fission yeast and insights made toward understanding those diseases (Wixon, 2002). It is a cylindrical cell that grows in a lengthwise direction and divides by splitting in the middle into two daughter cells, and its morphology and morphogenesis are generally well understood (Brunner, 2000; La Carbona, 2006). The width of *S. pombe* has been found to be controlled by the proteins Cdc42 (Kelly, 2011), Rga2 (Villar-Tajadura, 2008) and Rga4 (Das, 2007).

Also, many mutants of fission yeast have been generated to achieve a wide variety of purposes (Nasmyth, 1981; Forsburg, 2006; NBRP, 2014). Some of these include cell cycle checkpoint mutants that do not conduct the usual checks a cell performs in order to proceed successfully into the next stage of the cell cycle. One example is the Rad26 deletion (rad26Δ) strain designated 1001, which does not produce the Rad26 protein. Rad26 serves to respond to structural abnormalities of DNA and the microtubule cytoskeleton (al-Khodairy, 1994; De Souza, 1999; Baschal, 2006; Herring, 2010).

Many properties of fission yeast can be observed in order to understand toxin effects, including structural properties (Blasko, 2013). Cell size and morphology are easily measured properties that can reveal much about a cell's behavior, and morphology has been a useful indicator of responses to external stimuli (Mos, 2013). Fission yeast studies on common toxins have shown morphological changes consistent with expectations (Pyati, 2011). In particular, significant lengthening of cells has been observed upon exposure to phleomycin and hydroxyurea, two known drugs that damage DNA. As well, latrunculin A treatment has produced cells with decreased aspect ratio (width divided by length). Fission yeast studies have also revealed morphological effects of a variety of natural product toxins found in plants and other organisms (Heisler, 2014).

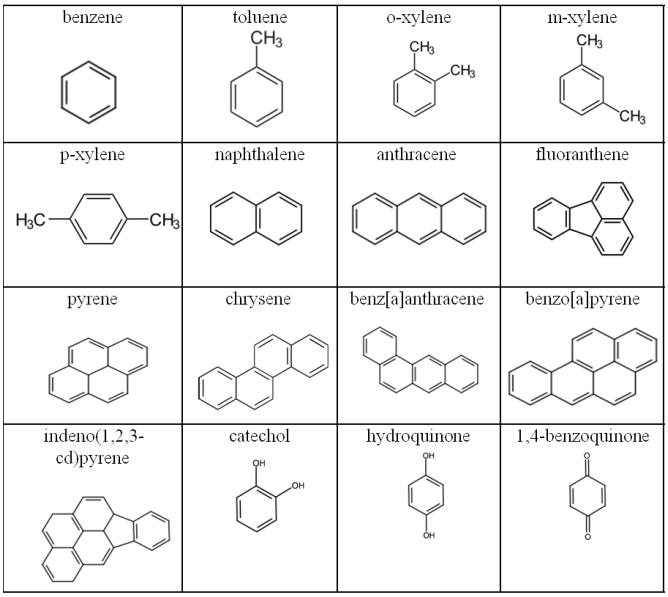

Figure 1. PAHs and related compounds studied in this work.

In this work, we reported the morphological effects on wildtype and rad26Δ fission yeast of several PAHs and related small molecules, measured by IFC. These molecules shown in Figure 1 include small molecule building blocks of PAHs, as well as related compounds found in tobacco smoke. The operating hypothesis of this study is that PAHs and related compounds affect the cells by either damaging the DNA or the cytoskeleton, and that the wildtype DNA detects this damage, whereas the rad26Δ strain does not.

This study was conducted using imaging flow cytometry. IFC enables the study of large populations of cells by acquiring tens of thousands of 2-D images in a few minutes using automated image capture and analysis. This allows a statistically rigorous analysis of populations than does traditional counting in a hemocytometer. In the IFC instrument used in this study, cells pass through a 50-mm flow cell and are observed and photographed through a 20x objective. Image analysis software measures and calculates parameters, such as cell length and width, for each image. It has been used to study other organisms such as cyanobacteria (Wert, 2013) and protozoa (Day, 2012).

MATERIALS AND METHODS

Chemicals

Anthracene (Matheson Coleman Bell, USA), benz[a]anthracene (Supelco, USA), benzene (Acros, USA), benzo(a)pyrene (Supelco, USA), 1,4-benzoquinone (Sigma-Aldrich, USA), catechol (Matheson Coleman Bell), chrysene (Sigma-Aldrich), fluoranthene (Supelco),

hydroquinone (Fisher, USA), indeno[1,2,3-cd)pyrene (Supelco), naphthalene (Fisher), pyrene (Sigma-Aldrich), toluene (Fisher), o-xylene (Fisher), m-xylene (Fisher) and p-xylene (Fisher) were used. Stock solutions of each toxin were prepared in dimethylsulfoxide (DMSO, Burdick & Jackson, USA). YE5S broth media was prepared from yeast extract (Becton Dickinson Bacto, USA), dextrose (anhydrous, BDH, USA), adenine hemisulfate dehydrate, (MP Biomedicals, Solon, Ohio, USA), L-histidine free base (MP Biomedicals), L-leucine (MP Biomedicals) and uracil (MP Biomedicals).

Strains and cell culture

S. pombe wild-type fission yeast with genotype leu1-32, ura4-d18,h, designated 236, and mutant strain with genotype rad26::ura^{+}, ura4-D18, leu1-32, ade6-704, h^{-}, designated 1001, were stored on YE5S agar slant media at 4°C. Reanimation of the yeast was accomplished in YE5S media broth with 24 h incubation at 30.5°C and a 120 rpm rotational shake.

Cell cultures were grown in a VWR Incubator (Sheldon Manufacturing, Cornelius, OR) at 30.5°C and a 120 rpm rotational shake function for liquid solutions. Optical densities at 595 nm (OD_{595}) were recorded with a blank of YE5S. Following starter culture, transfer volumes and growth times for final samples were controlled in order to obtain OD_{595} values between 0.2 and 0.9. The transfer volume ($V_{transfer}$) was calculated using the OD_{595} obtained from the starter culture and the formula below:

$$V_{transfer} = \frac{0.3}{OD_{actual}} \frac{1}{2^{N-1}} * V_{final} \quad where\ N = \frac{t_{incub}}{t_{gen}}$$

The calculated $V_{transfer}$ was added into 5 mL of YE5S media and incubated at 30°C and 120 rpm for a minimum of 12 h. Following this growth period, OD_{595} was measured again. If OD_{595} exceeded 0.3, the sample was diluted with YE5S in order to achieve an OD_{595} of 0.3, to ensure that plateau growth and senescence did not occur during the 6-hour period of toxin exposure. Each individual toxin was then added to a triplicate group of cultures to yield a final toxin concentration of 10 µM. Control samples did not have any toxin added but underwent the same OD_{595} measurement, dilution and 6-hour growth period. OD_{595} was measured once more; all final OD_{595} values were between 0.2 and 0.9 and were higher than the OD_{595} measured before toxin incubation. The samples were centrifuged at 5000 rpm for 2 min, washed in phosphate buffered saline (PBS, 0.2 M phosphate, 1.5 M NaCl), aspirated, centrifuged again and resuspended in 70% cold ethanol to preserve samples. The samples were stored at 4°C until ready for flow cytometric analysis.

Imaging flow cytometry

Samples in ethanol were resuspended in phosphate buffered saline (PBS) prior to IFC analysis. Samples underwent two cycles of the following: centrifugation at 5,000 rpm for 2 min, removal of supernatant, dilution in PBS, aspiration and vortexing to break up cell clumps. Final samples in PBS were allowed to incubate for 30 min prior to flow cytometric analysis.

Two-dimensional fission yeast cell images were collected with a FlowCAM Imaging Flow Cytometer (IFC), 20x microscope objective, and 50 mm flow cell (Fluid Imaging Technologies, Yarmouth, ME). Eight to ten drops of the sample solution was placed into the opening of the FlowCAM IFC and 75,000 images were collected using FlowCAM VisualSpreadsheet software version 3.4.5. A post capture filter, a filter that contains ranges of five parameters that reflect single cell images, was used to filter the raw image files of all the PAHs and control samples. The postcapture filter was validated using established observations and consisted of the following: Circle Fit 0.2 - 2.0, Circularity 0.4 - 4.0, Fiber Curl 0.0 - 0.2, Fiber Straightness 0.7 - 4.0 and Symmetry 0.75 - 2.0. FlowCAM software eliminated images that did not have values within those parameters set by the filter, resulting in a refined set of predominantly acceptable images. All samples have a minimum of 10,000 acceptable images.

Data analysis

A table containing parameters for each cell was exported to Microsoft Excel. The two parameters of interest in this work were length and width; mean values of these were calculated in Excel. Triplicate trials of each experiment yielded average values and standard deviations for both mean length and width. Error for a set of triplicate was calculated using a partial derivative formula (Mortimer, 1981).

RESULTS AND DISCUSSION

Figure 2 shows a representative sample of images. For comparison purposes, each panel is drawn from images having approximately the same length range. Panel A shows images in the 6 mm range from strain 236 exposed to chrysene, and Panel B shows images in the same length range for untreated cells as a control. The width values are lower in the chrysene images than in the control images, in this sample set of images. While it is difficult to visually estimate changes in length or width, this image is a very small representative sample of the full data set of 10,000 images for each experiment. The comprehensive analysis presented in Table 1 includes the full data set.

For the group of experiments as a whole, mean absolute length values fell between 5.1 and 6.3 µm. Mean absolute width values fell between 2.3 and 3.2 µm. Absolute values for length and width are subject to day-to-day variations in growth behavior, so all length and width data is presented relative to a control experiment growing under the same conditions with no toxin. Table 1 shows the results of the mean for three trials for L/Lc, where Lc stands for Lcontrol, and W/Wc, where Wc stands for W control, in percentages. Results for wildtype 236 for known drugs are also included (Pyati, 2011). A result of 100% means that no change from control is observed.

Several observations are clear from the results in Table 1. First, for all toxins, L/Lc is at or very close to 100%, meaning that none of the treatments served to lengthen the cells relative to control. This is a marked difference from treatment by phleomycin and hydroxyurea, two known genotoxins that have been shown to lengthen yeast cells (Pyati, 2011; Belenguer, 1995). Each of these operates in its own manner: phleomycin acts to create DNA breaks, (Sleigh, 1977) whereas hydroxyurea prevents DNA synthesis (Bianchi, 1986). Nevertheless, the morphological effects of phleomycin and hydroxyurea are not observed upon exposure to this set of PAHs, indicating that the mechanism of action for these PAHs in

A. Chrysene-exposed 236 yeast cell images.

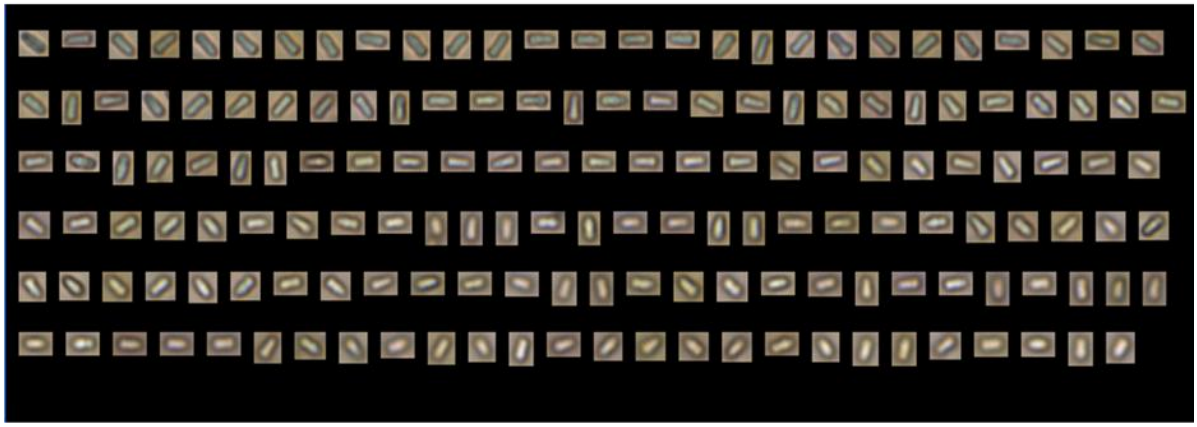

B. Control 236 yeast cell images.

Figure 2. Images collected with FlowCAM IFC. Panels contain images in the same length range from each representative sample, for comparison. (a) *S. pombe* 236 strain cells subjected to chrysene, lengths ranging from 6.05-6.12 mm and widths ranging from 1.46- 3.87 mm. (b) S. pombe 236 strain cells subjected to no toxin as a control, lengths from 6.05-6.11 mm and widths from 1.70-4.11 mm.

fission yeast is different from those of phleomycin and hydroxyurea.

Second, a clear decrease in cell width for wildtype 236 yeast is observed upon exposure to the following group of five toxins: chrysene, fluoranthene, o-xylene, indeno-(1,2,3-cd)pyrene, and naphthalene. These cells exhibit essentially the same length as control, but their widths are lowered. Chrysene exhibits the lowest width of all: 73.1% of control. This suggests a mechanism whereby these toxins affect cytoskeletal structures that determine the width of a cell. This decrease in width is observed only in the wildtype 236 strain. The 1001 strain does not detect the problem and continues replicating with an impairment.

Cell width has been shown to be controlled by small GTPases such as Cdc42, Rga2, and Rga4. Cdc42 has been shown to have multiple effects on cell width (Kelly, 2011). Via one pathway, deletion of Cdc42 guanine nucleotide exchange factors Scd1 and Scd2 has been shown to reduce cellular levels of Cdc42 and yield wider cells. Via a separate pathway, deletion of Cdc42 GTPase activating protein Rga4 resulted in increased Cdc42 and produced wider cells. So this work demonstrated that while both increased and decreased Cdc42 levels resulted in wider cells, each of these two mechanisms worked separately in different parts of the cell. Factors that cause reduced cell width was not observed in this work, although reference was made to other studies in which cell width was reduced. These studies have included other small GTPases, particularly Rga2 and Rga4. Reduced cell width has resulted from over-expression of Rga4, whereas deletion of rga4 yields

Table 1. Mean length and width relative to control of wildtype 236 and rad26Δ 1001 mutant fission yeast exposed to PAHs and related compounds.

Toxin	Yeast strain	L/Lc (%)[1]	W/Wc (%)[2]
Effects on 236 but not 1001			
236 less wide			
Chrysene	236	100.7 ± 11.4	73.1 ± 8.7
	1001	107.0 ± 4.4	103.9 ± 4.0
Fluoranthene	236	100.0 ± 6.1	75.3 ± 9.0
	1001	101.5 ± 8.4	102.1 ± 11.6
O-xylene	236	97.7 ± 8.6	77.5 ± 8.8
	1001	102.9 ± 4.4	100.8 ± 5.9
Indeno-(1,2,3-cd)pyrene	236	94.6 ± 6.9	79.4 ± 14.5
	1001	105.4 ± 5.4	98.2 ± 3.2
Naphthalene	236	103.3 ± 5.3	85.6 ± 10.4
	1001	102.9 ± 4.2	103.3 ± 2.2
236 wider			
Benzo(a)pyrene	236	101.0 ± 5.4	106.7 ± 2.6
	1001	99.1 ± 1.9	98.9 ± 2.8
P-xylene	236	105.3 ± 20.9	107.5 ± 6.6
	1001	101.2 ± 4.4	98.2 ± 3.6
No effects			
Anthracene	236	93.3 ± 13.7	98.7 ± 9.5
	1001	104.2 ± 4.7	104.5 ± 1.9
Benz(a)anthracene	236	97.7 ± 10.5	99.0 ± 13.0
	1001	103.0 ± 4.7	100.5 ± 2.4
1,4-Benzoquinone	236	102.1 ± 9.8	100.0 ± 5.3
	1001	105.1 ± 4.7	96.8 ± 3.7
Hydroquinone	236	100.4 ± 9.6	100.8 ± 6.3
	1001	103.4 ± 4.5	101.6 ± 2.3
Toluene	236	101.1 ± 20.9	101.2 ± 9.6
	1001	103.5 ± 4.3	98.1 ± 6.2
M-xylene	236	103.9 ± 20.8	101.3 ± 7.8
	1001	101.5 ± 4.4	101.1 ± 2.8
Benzene	236	103.9 ± 20.6	101.8 ± 8.6
	1001	97.6 ± 7.0	95.8 ± 6.7
Pyrene	236	97.4 ± 18.5	105.6 ± 7.7
	1001	105.8 ± 5.2	100.5 ± 3.8
Catechol	236	110.2 ± 23.5	105.9 ± 8.7
	1001	98.7 ± 4.6	95.6 ± 4.2
236 with known drugs			
Phleomycin		156.0	96.2
Hydroxyurea		109.3	104.7
Latrunculin A		115.4	110.5

[1]L/Lc = mean length divided by mean length of control, in percent form;
[2]W/Lc = mean width divided by mean width of control, in percent form.

wider cells (Das, 2007). Conversely, thinner, longer cells have resulted from deletion of rga2, whereas Rga2 overexpression produced shorter, broader cells (Villar-Tajadura, 2008). Clearly small GTPases play an essential

role in control of cell width. It is possible that the five hydrocarbons causing marked reductions in cell width in this study may be playing a role regarding the expression, function, or activation of Cdc42, Rga2, or Rga4.

Another possibility is that the effects of these toxins accompany formation of the contractile actinomyosin ring that is formed in early anaphase. This bears an interesting similarity to the toxin latrunculin A, a drug known to depolymerize actin structures (Liu, 2000; La Carbona, 2006). Previous experiments on latrunculin A effects on fission yeast have shown that the aspect ratio decreases relative to control for strain 236. The latrunculin A results in Table 1 indicate increases in both length and width relative to control, but width decreases to a greater extent. This yields a decrease in aspect ratio of 9.2% (Pyati, 2011), or a narrowing of the cell. This narrowing is comparable to the behavior of this set of PAH toxins. This suggests that this group of PAH toxins may serve to depolymerize actin, like latrunculin A, thus limiting the size of the contractile actinomyosin ring, among other effects.

In addition, there are some slight effects observed in some other toxins. Benzo(a) pyrene and p-xylene show a slightly wider 236 cell, at 106.7 and 107.5% of control respectively, although not to the extent observed in the first group of less wide cells. Anthracene shows a wider cell in 1001, at 104.5% of control, but again to a very small extent.

The lack of significant effects exerted by benzo(a)pyrene is a significant finding, because benzo(a)pyrene is one of the most toxic PAHs (Crosby, 1998). This suggests a mechanism distinct from the usual mechanism of benzo(a)pyrene toxicity: formation of a diol-epoxide and consequent formation of a DNA adduct (Beland, 1994). This finding lends strength to the argument that changes to fission yeast morphology reported here do not occur via DNA damage, but rather, by another mechanism.

As well, the chemical structural requirement for this mechanism, referred to as a “bay region,” appears not to be a requirement for the mechanism of cellular change observed in this study. This bay region, illustrated in Figure 3, is known to increase the biochemical reactivity of PAHs by facilitating the formation of the diol-epoxide (Baird, 2008). Therefore, other species with bay regions may not necessarily show changes in cell width in this study.

Several toxins have no effect on morphology: these are benz(a)anthracene, 1,4-benzoquinone, hydroquinone, toluene, m-xylene, benzene, pyrene and catechol. Some of these are quite water-soluble, such as catechol and hydroquinone, and are likely excreted rapidly by cells. Others, like toluene, m-xylene, pyrene and 1,4-benzoquinone, are not known to possess high toxicity or carcinogenicity. The most surprising among these are benz(a)anthracene and benzene, both of which are known carcinogens. Clearly, these compounds must address pathways separate from morphology that produce cancerous phenomena. Benz(a)anthracene does possess a bay region, but this structural feature is not essential in the activity of PAHs found in this study.

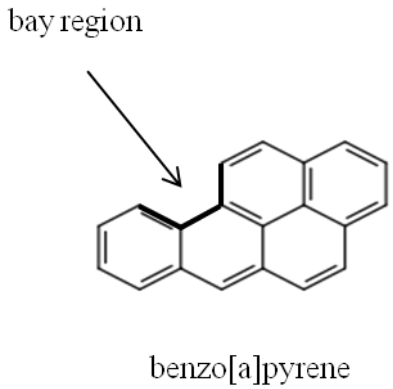

Figure 3. Benzo(a)pyrene with bay region illustrated by dark lines.

Finally, the rad26D mutant 1001 also displays no effects caused by these molecules. Rad26 is known to be essential to both DNA checkpoint signaling and to microtubules, so use of this mutant enables the study of whether the DNA checkpoint or the microtubules are affected. In terms of DNA, a Rad26/Rad3 complex detects DNA damage by a mechanism not fully understood, and then the Rad26 participates in the cell cycle arrest and repair of DNA (Wolkow, 2003). Also, Rad26 plays a role regarding microtubules: rad26Δ cells are unable to correctly complete two processes that depend on microtubules: chromosome segregation and morphogenesis (Baschal, 2006). The lack of effects by these compounds on the rad26Δ mutant adds support to the idea that they are not affecting DNA structure or microtubules.

Conclusions

This study shows that the cell width of wildtype fission yeast is significantly reduced by five toxins: chrysene, fluoranthene, o-xylene, indeno-(1,2,3-cd)pyrene and naphthalene. The cause of this bears further investigation and likely involves small GTPases such as Cdc42, Rga2, and Rga4, as well as the cell’s actin ring. The chemical structures of these molecules possess some similarities but are quite similar to other toxins exhibiting no effect in this work. Clearly, the bay region is not a critical structural element to this effect.

It is even possible that there are some causality in the other direction, that is, changes in cell morphology are part of the cause of carcinogenesis, instead of morphology’s simply being a second symptom of a primary pro-

blem induced by the toxin. This causal link between morphology change and cancer development has been found in another work (Hall, 2009).

Conflict of Interest

The authors have no financial or other interest that would influence the results of the study.

ACKNOWLEDGEMENT

The University of North Florida is acknowledged for financial support.

REFERENCES

al-Khodairy F, Fotou E, Sheldrick KS, Griffiths DJ, Lehmann AR, Carr AM. (1994). Identification and characterization of new elements involved in checkpoint and feedback controls in fission yeast. Mol. Biol. Cell. 1994 Feb; 5(2):147-60.

Alnafisi A., Hughes J, Wang G, Miller CA 3rd. (2007) Evaluating polycyclic aromatic hydrocarbons using a yeast bioassay. Environmental Toxicology and Chemistry 26(7):1333-1339.

Baird C, Cann M. (1998). Environmental Chemistry 4th Edition, WH Freeman: New York. pp. 514-515.

Baschal EE, Chen KJ, Elliott LG, Herring MJ, Verde SC, Wolkow TD (2006). The fission yeast DNA structure checkpoint protein RAD26ATRIP/LCDI/UVSD accumulates in the cytoplasm following microtubule destabilization. BMC Cell Biol. 7:32.

Beland FA, Poirier MC. (1994). DNA adducts and their consequences. Methods to assess dna damage and repair: interspecies comparisons. Tardiff RD, Lohman PHM, Wogan GN ed. Scope-John Wiley and Sons: 29-55.

Belenguer P, Oustrin M, Tiraby G, Ducommun B (1995). Effects of phleomycin-induced DNA damage on the fission yeast *Schizosaccharomyces pombe* cell cycle. Yeast 11:225-231. PMID:7785323.

Bianchi V, Pontis E, Reichard P (1986). Changes of deoxyribonucleoside triphosphate pools induced by hydroxyurea and their relation to DNA synthesis. J. Biol. Chem. 261:16037-16042.

Blasko A, Mike N, Grof P, Gazdag Z, Czibulya Z, Nagy L, Kunsagi-Mate S, Pesti M (2013). Citrinin-induced fluidization of the plasma membrane of the fission yeast *Schizosaccharomyces pombe.* Food Chem. Toxicol. 59:636-642.

Brunner D, Nurse P (2000). New concepts in fission yeast morphogenesis. Phil. Trans. R.Soc. Lond B 355, 873-877.

Chaudhuri SP, Sundaram G., Bhattacharya A, Ray P, ray A, Chatterjee IB, Chattopadhyay D (2005). Activation of S phase checkpoint by cigarette smoke extract in *Schizosaccharomyces pombe*. Yeast 22:1223-1228.

Chramostova K, Vondracek J, Sindlerova L, Vojtesks B., Kozubik A, Machala M (2004). Polycyclic aromatic hydrocarbons modulate cell proliferation in rat hepatic epithelian stem-like WB-F344 cells. Toxicol. Appl Pharmacol. 196:410-421.

Crosby DG (1998). Environmental Toxicology and Chemistry. Oxford University Press: New York. p. 254.

Das M, Wiley DJ, Medina S, Vincent HA, Larrea M, Oriolo A, Verde F (2007). Regulation of cel diameter, For3p localization, and cell symmetry by fission yeast Rho-GAP Rga4p. Mol. Biol. Cell 18:2090-2101.

Day JG, Thomas NJ, Achilles-Day UE, Leakey RJ (2012). Early detection of protozoan grazers in algal biofuel cultures. Bioresour. Technol. 114:715-719.

De Souza CP, Ye XS, Osmani SA (1999). Checkpoint defects leading to premature mitosis also cause endoreplication of DNA in *Aspergillus nidulans*. Mol. Biol. Cell 10:3661-3674.

Deng Y, Zhang Y, Hesham A, Liu R, Yang M (2010). Cell surface properties of five polycyclic aromatic compound-degrading yeast strains. Appl Microbiol Biotechnol 86(6):1933-9.

Forsburg S, Rhind N. (2006). Basic methods for fission y east. Yeast 23:173-180. http://dx.doi.org/10.1002;yea.1347.

Hall A. (2009). The cytoskeleton and cancer. Cancer Metastasis Rev. 28:5-14.

Heisler J, Elvir L, Barnouti F, Charles E, Wolkow TD, Pyati R (2014). Morphological effects of natural products on schizosaccharomyces pombe measured by imaging flow cytometry. Nat. Prod. Bioprospecting. 4(1):27-35.

Herring M, Davenport N, Stephan K, Campbell S, White R, Kark J, Wolkow TD (2010). Fission yeast RAD26ATRIP delays spindle-pole-body separation following interphase microtubule damage. J. Cell Sci. 123(9):1537-45.

Kelly FD, Nurse P (2011). , Spatial control of Cdc42 activation determines cell width in fission yeast. Mol. Biol. Cell 22:3801-3811.

La Carbona S, Le Goff C, LeGoff X. (2006). Fission yeast cytoskeletons and cell polarity factors: connecting at the cortex. Biol. Cell 98:619--631.

Liu J, Wang H, Balasubramanian , MK .(2000). A checkpoint that monitors cytokinesis in Schizosaccharomyces pombe. J. Cell Sci. 113:1223-1230.

Mortimer RG. (1981). Mathematics for Physical Chemistry; Macmillan Publishing: New York: 280.

Mos M, Esparza-Franco MA, Godfrey EL, Richardson K, Davey J, Ladds G (2013). The role of the RACK1 ortholog Cpc2p in modulating pheromone-induced cell cycle arrest in fission yeast. PLOS One 8(7): e65927. doi:10.1371/journal.pone.0065927.

Munoz B, Albores A. (2011). DNA damage caused by polycyclic aromatic hydrocarbons: mechanisms and markers, selected topics in DNA repair. Chen D ed. In Tech, http://www.intechopen.com/books/selected-topics-in-dna-repair/dna-damage-caused-by-polycyclic-aromatic-hydrocarbons-mechanisms-and-markers.

Nasmyth K, Nurse P (1981). Cell division cycle mutants altered in DNA replication and mitosis in the fission yeast Schizosaccharomyces pombe. Mol Gen Genet 182(1):119-24. http://dx.doi.org/10.1007/BF00422777.

NBRP National BioResource Project (Yeast), (2014). http://yeast.lab.nig.ac.jp/nig/index_en.html, accessed May 29, 2014.

Pyati R, Elvir LL, Charles, CE, Seenath U, Wolkow TD. (2011). Imaging flow cytometric analysis of *Schizosaccharomyces pombe* morphology. J. Yeast Fungal Research 2(7):106-112.

Rubin H (2001). Synergistic mechanisms in carcinogenesis by polycyclic aromatic hydrocarbons and by tobacco smoke: a bio-historical perspective with updates. Carcinogenesis 22(12):1903-1930.

Siebert D, Marquardt H, Friesel H, Hecker E (1981). Polycyclic aromatic hydrocarbons and possible metabolites: convertogenic activity in yeast and tumor initiating activity in mouse skin. Cancer Res. Clin. Oncol. 102(2):127-139.

Sleigh MJ, Grigg GW. (1977). Sulphydryl-mediated DNA breakage by phleomycin in *Escherichia coli*. Mutat. Res. 42:181-190.

Sundaram G, Palchaudhuri A, Chaudhuri S, Karunanithi S., Chattopadhyay D. (2008a). Characterization of Sro1, a novel stress responsive protein in *Schizosaccharomyces pombe*. FEMS Yeast Res. 8:564-573.

Sundaram G, Palchaudhuri S, Dixit S, Chattopadhyay D. (2008b). MAPK mediated cell cycle regulation is associated with Cdc25 turnover in S. pombe after exposure to genotoxic stress. Cell Cycle 7(3):365-372.

Talhout R, Schulz T, Florek E, van Benthem J, Wester P, Opperjuizen A (2011). Hazardous compounds in tobacco smoke. Int. J. Environ. Res. Public Health 8:613-628.

USEPA (2014). Priority Pollutants, United States Environmental Protection Agency. http://water.epa.gov/scitech/methods/cwa/pollutants.cfm. Accessed May 27, 2014.

Villar-Tajadura MA, Coll PM, Madrid M, Cansado J, Santos B, Perez P (2008). Rga2 is a Rho2 GAP that regulates morphogenesis and cell integrity in *S. pombe*. Mol. Microbiol. 70(4):867-881.

Wert EC, Dong MM, Rosario-Ortiz FL (2013). Using digital flow cytometry to assess the degradation of three cyanobacteria species after oxidation processes. Water Res. 47(11)3752-3761.
Wixon J. (2002). Featured organism: schizosaccharomyces pombe, the fission yeast. Comparative and Functional Genomics 3(2):194-204.
Wolkow TD, Enoch T (2003). Fission yeast Rad26 responds to DNA damage independently of Rad3. BMC Genetics 4:6-16.